Biomaterials Science: Processing, Properties and Applications III.
Edited by Susmita Bose, Amit Bandyopadhyay and Roger Narayan.

EFFECT OF COLD WORK AND AGING ON A COBALT-NICKEL BASED ALLOY

S. Cai
Fort Wayne Metals Research Products Corporation, 9609 Ardmore Ave., Fort Wayne, In 46809

A.T.W. Barrow
Dept. of Mechanical and Materials Engineering, Queen's University, Nicol Hall, 60 Union Street, Kingston, Ontario, Canada K7L 3N6

R. Yang
Argonne National Laboratory, 9700 S. Cass Ave, 433/D008, Argonne, Il 60439

L.E. Kay
Fort Wayne Metals Research Products Corporation, 9609 Ardmore Ave., Fort Wayne, In 46809

ABSTRACT

Cobalt-nickel based MP35N (35Co, 35Ni, 20Cr, 10Mo) alloy is characterized by a combination of extremely high strength, high toughness, corrosion resistance and ductility. In this study, experiments were carried out to investigate the influence of cold work and aging treatment on its mechanical properties. An annealed material was cold worked to 30-90% reduction and aged at temperatures from 400 to 700°C for 10 minutes to 16 hours. It is found that this material work hardened rapidly with strength almost doubled after 30% cold work. Aging provides a secondary strengthening, which depends on the aging temperature and previous cold work level. An excellent combination of mechanical properties can be obtained from the material with 75%cw and aged at ~500°C for 2-4 hours, where the Yield Strength (Y.S) larger than 2000MPa, the Ultimate Tensile Strength (UTS) above 2200MPa and the Reduction of Area (RA) ~40% can be achieved. TEM observations and synchrotron X-ray diffractions suggest the work hardening is caused by the increased density of dislocations, the development of the <111> and <100> texture and the deformation twins, while the secondary age hardening is associated with the increased number of micro-twins produced during the aging process.

INTRODUCTION

Cobalt-nickel based multiphase (MP) alloys, originally developed by G.D. Smith [1], are characterized by a unique combination of ultrahigh strength, high ductility and toughness, and excellent oxidation and corrosion resistance. Among them, MP35N (35Co, 35Ni, 20Cr, 10Mo) alloy has been widely used in aerospace, marine, petro-chemical [2] and food process [3] industries for years and recently in medical applications such as orthopedic implants [4], guide wires [5] and pace maker leads [6] due to its non-magnetic feature and biocompatibility in addition to the high strength and toughness[4]. After anneal, this alloy is a single phase material with a FCC crystal structure. It work harden rapidly during deformation to very high strength, while still maintaining good ductility (e.g. UTS ~1700MPa and RA >40% after ~60% cold work) [1,3]. Secondary strengthening can be obtained by heat treating materials with cold work above certain level [7,8], which distinguishes it from the regular precipitation hardening process. Although this material has been used in many critical applications for many years, only few studies have been carried out regarding its deformation mechanism and heat treating responses, and explanations to some of the experimental observations are still controversial. For example, the rapid work hardening was first attributed to the stress or strain induced phase transformation, by which thin HCP platelets were formed in the FCC matrix during deformation [1]. According to G.D. Smith [1], after the annealed material was cold rolled to 80% reduction, it had approximately 30% HCP phase. This was later supported by the TEM analysis of A.H. Graham et al. [9] in a material with a similar process history. The presence of HCP platelets was also observed by R.P. Singh and R.D. Doherty in materials after cold drawn to ~48% deformation [10]. However, people from the same group later reported that no HCP phase was seen in samples compressed to ~0.7 true strain (~50% engineering strain) and proposed that the strain induced martensite plays no role in the room temperature deformation [11]. Similar observation was reported by M. Raghavan and his colleagues on materials with 59% cold work [12]. They proposed that the strain induced phase transformation temperature, M_d, depends on the chemistry; for alloys with higher cobalt content (e.g. >50 wt%), the M_d, is above room temperature, therefore these alloys experience strain induced martensite transformation during room temperature deformation. While for alloys with lower cobalt content, such as MP35N, the M_d is much lower than room temperature and thus only dislocation slip and deformation twinning occur during room temperature deformation [13]. Compare to the work hardening, the mechanism of the age hardening appears to be well established. Graham [14] first suggested that the age hardening is caused by the partitioning of solute elements between the FCC and HCP phases during aging, where Mo and Cr go to HCP phase, while the FCC phase become more Ni enriched. This idea was supported by R. P. Singh et al. [10] and further improved by S. Asgari et al. [8], who proposed that the segregation of solute elements and high dislocation density promote the formation and growth of thin HCP precipitates, and thus produce large secondary hardening during aging.

Since most of the previous studies worked on materials with cold work less than 60%, it is still hard to believe the stress induced phase transformation is not an active deformation mode in this material. It may only occur at high cold work level (e.g. ~80%), while at low strain level (e.g. <50%), only deformation twinning or dislocation slip will be activated. Obviously, experiments with cold work larger than 80% will help to clarify this hypothesis. One useful technique to understand the deformation behavior is to study the texture evolution during deformation as the texture change is directly correlated to the deformation mechanism. However, very few texture measurements have been carried out on this material to date. A. Ishmaku et al. [15] reported a {110} fiber textures developed in materials cold rolled to 80% reduction. B.Q. Li et al. [6] reported a strong <111> and weak <100> texture in the cold drawn condition. Recently, a new process developed by Fort Wayne Metal is found to produce a strong <100> texture in the wire axial direction [16]. The advantage of this texture distribution is that it largely reduces the Young's modulus and thus increases the elastic strain. Materials with low Young's modulus and large elastic strain are highly demanded for medical applications such as orthodontic arch wires and guide wires. However, how this texture was developed remains unanswered. Clearly, despite of its importance, researches conducted on MP35N alloy is not enough, and our knowledge on its deformation mechanism is still very limited. In this paper, we report our recently study on the influence of cold work and aging treatment on the mechanical properties of MP35N alloy. In this study, an annealed material was cold drawn to over 90% reduction and then aged at temperatures from 400 to 700°C for 10 minutes to 16 hours. While the mechanical properties such as strength and elongation were tested for an understanding of the influence of processing. The microstructures and textures before and after heat treatment were studied by TEM and Synchrotron X-ray diffraction.

MATERIAL AND EXPERIMENTS

The material used in this study was made by Carpenter Technology. It consists of 35.27Ni, 20.52Cr, 9.43Mo, 0.74Ti, 0.12Fe, 0.007C and balanced Co (wt%). This material was repeatedly annealed at 926°C for 1 hour and cold drawn by ~30%, 50%, 75% and 90% reduction to a finish diameter of ~3mm. Wires with difference amount of cold work were then rotary straightened and cut into 35cm long bars, which were then heat treated in a lab furnace at temperatures from 400 to 700°C for time from 10 minutes to 16 hours and water quenched to room temperature. The temperature variation in furnace is ~6°C. Heat treated bars were ground by 200μm to get rid of the surface oxide. Tensile test was carried out on an Instron tensile tester with a load cell of 10K pounds capacity. During the test, samples were first loaded at a strain rate of 0.007 per minute to 3% engineering strain, after which the strain rate is increased to 0.1 per minute. The sample gauge length is 254mm. The deformation strain was measured by an extensometer attached on the sample. The yield strength is defined by 0.2% offset method. The Micro-hardness was tested on areas close to the center of the wire along the axial wire direction with a testing load of 200 grams. 6 to 10 tests were carried out on each sample.

Thin-foil samples were prepared by taking 0.15mm slices along the axial direction and mechanically thinning to 50 μm using 1200 grit SiC paper. Foils were electropolished in a solution of 19% H_2SO_4 and 6% H_3PO_4 in 75% methanol (by volume) using a Struers Tenupol 5. Optimum conditions were achieved at a temperature of 4±1°C and a voltage of 21 V, and gave a current of 28-30 mA. Transmission electron microscopy was carried out on a Philips CM20 at an accelerating voltage of 200 kV.

X-ray diffraction was carried on the beam line 11-ID-C at the Advanced Photon Source (APS) at Argonne National Laboratory. A monochromatic X-ray beam with a wavelength 0.10801°A was used. The beam size is 0.5×0.5mm^2. The experimental set-up is similar to that shown in [19]. The raw 2D X-ray images were interpreted by Fit2D software [20] to generate 72 diffraction spectra along the 360 degree azimuth angle. These diffraction spectra were fitted by the Rietveld refinement in Maud [21] software to calculate the texture. Also, diffraction spectra at certain azimuth angles (such as those parallel and perpendicular to the bar axial direction) were input in GSAS [22] to fit the individual peak position, intensity and peak broadening, etc.

RESULTS AND DISCUSSIONS

EFFECT OF COLD WORKING ON MECHANICAL PROPERTIES

Figure 1 shows the influence of cold work on mechanical properties. Clearly, both the Y.S and the UTS increased rapidly by cold working; the Y.S and UTS both were doubled after ~50% cold work. On the other hand, the RA decreased with increasing cold work. Assuming a linear relationship, the UTS and the Y.S was increased by 14 and 15MPa with 1% deformation respectively, while the RA was decreased by ~0.4%. A very similar relationship can be found in [3]. After 90% cold work, an excellent combination of high strength and ductility was obtained with the UTS of ~2300MPa and the RA close to 40%.

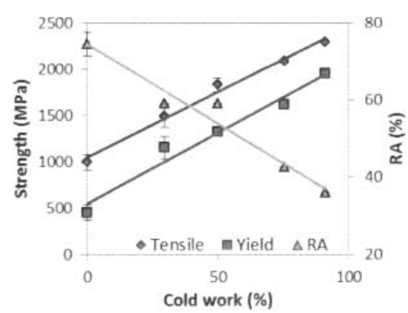

Figure 1 Effect of cold work on mechanical properties

EFFECT OF AGING ON MECHANICAL PROPERTIES

The influences of aging treatment on mechanical properties are plotted in Figs. 2 to 5. It is worth to note that the starting points in Figs.2-5 represent the properties in the "as straight" condition, which is different from those in the "as drawn" condition represented by dashed lines in Figs. 2-5. This is due to the Bauschinger effect caused by the rotary straightening process as the deformation path was changed from cold drawn process to straightening process [17].

Fig.2 shows the change in the Y.S after aging at different temperatures and time. Several features are in common for all the materials with different amount of cold work;

1. The Bauschinger effect caused by the rotary straightening was quickly recovered by aging. After aging for 10 minutes, almost all samples have the Y.S even higher than that in the "as drawn" condition.
2. Age strengthening increased with increasing the amount of cold work up to 75%CW. For the material with 30% cold work, the largest increment in the Y.S was ~150MPa after aged at 500°C. For material with 50% and 75% cold work, it was ~500MPa. For the material with 90% cold work, the largest increment was about 400MPa, which resulted in the highest Y.S of ~2300MPa.
3. The strength increment is more temperature dependent and less time dependent. The largest age strengthening was obtained at temperature of ~500°C. Also, it can be seen that the increment in the Y.S was mostly obtained within 1 to 2 hours of aging; further increasing aging time didn't result in significant changes.

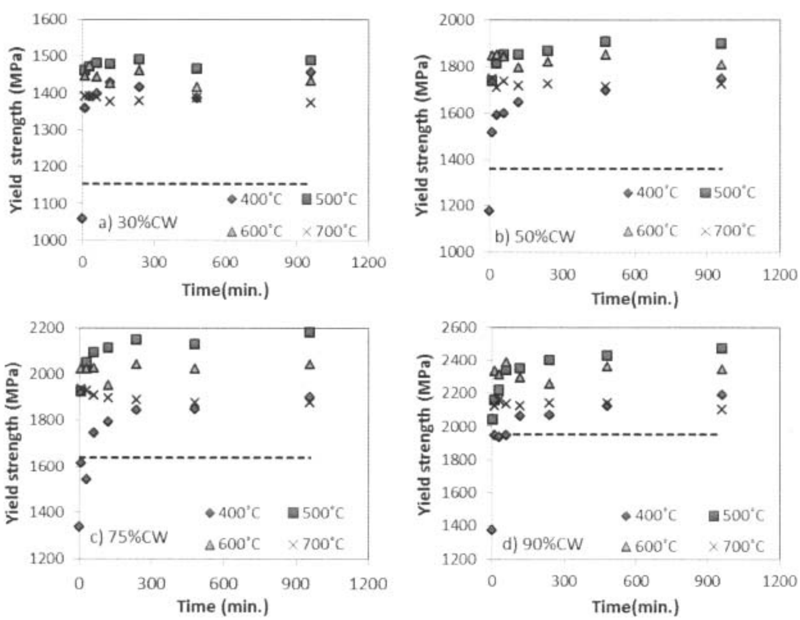

Figure 2 Yield strength after aging at different temperatures and time. Dashed lines represent the Y.S in "as drawn" condition. Errors are less than 70MPa.

Similar to the Y.S, the influence of aging on the UTS was mostly active within the first 2 hours, and further increasing the aging time didn't produce too much difference. Also, the increment in the UTS is mostly relied on the previous cold work level and the aging temperature as shown in Fig, 3. It can be seen that at the same cold work level, the highest UTS after heat treatment was achieved at 500°C. At the same temperature, the strength increment increases with the previous cold work level. The UTS in materials with 75% and 90%CW was increased by ~500MPa to a value of 2300 and 2500MPa respectively after aged at 500°C. Correspondingly, the hardness after aging is also increased with the cold work level (Fig.4). For materials with 30%CW, the hardness after aging is almost the same as that before aging. For materials with 50 to 75%CW, the hardness reached to ~600Hv after aging. While for those with 90%CW, after aging at 500 and 600°C, their hardness was increased by ~120Hv to around 680Hv.

The large increase in strength was accompanied by a decrease in ductility. From Fig.5 it can be seen that when the cold work is low (i.e. <75%), aging didn't cause big change in the RA. All samples were able to maintain the similar RAs to those before aging treatment. For samples with 75%CW, the RA was slightly deceased to ~40% after aged at 500°C for 4 hours, providing a good combination of strength and toughness. While, for samples with 90%CW, aging at 500°C decreased the RA to near zero; and the fracture surface had a shear-type morphology at an angle of ~45° to the tensile loading direction as shown by Fig.4b in reference [7].

EFFECT OF COLD WORK AND AGING ON MICROSTRUCTURES

The microstructures of cold worked materials are shown in Fig. 6. Generally, all samples show similar microstructures that consist of lot of diffraction contrast from the homogeneous distribution of dislocations, intersected planar dislocation arrays and deformation twins (Fig.6a-b). In the center of Fig.6a, twins dissected planar deformation bands, implying that deformation twinning occurred later in the process. These features are typical of deformed Low SFE *FCC* metals and consistent to that in [10]. With increasing cold work, more intersected planar dislocations and deformation twins were formed (Fig.6c); and planar deformation was also seen in many of the deformation twins. Some very thin stacking faults

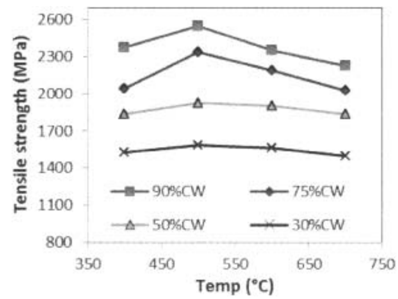

Figure 3 Tensile strength after aging at different temperatures for 4 hours. Errors are less than 100MPa.

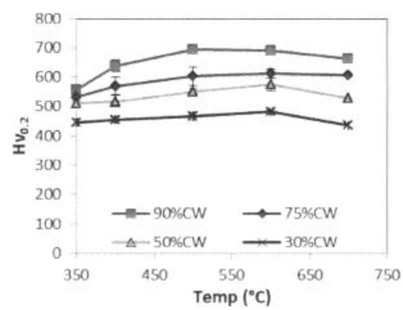

Figure 4 Hardness after aging at different temperatures for 4 hours. Hardness at 350°C represents the value before aging.

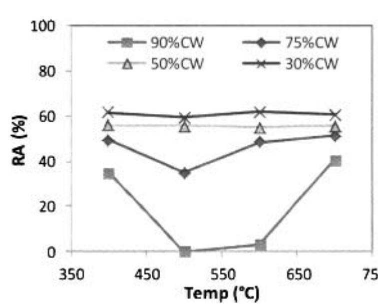

Figure 5 Reduction of area after aging at different temperatures for 4 hours.

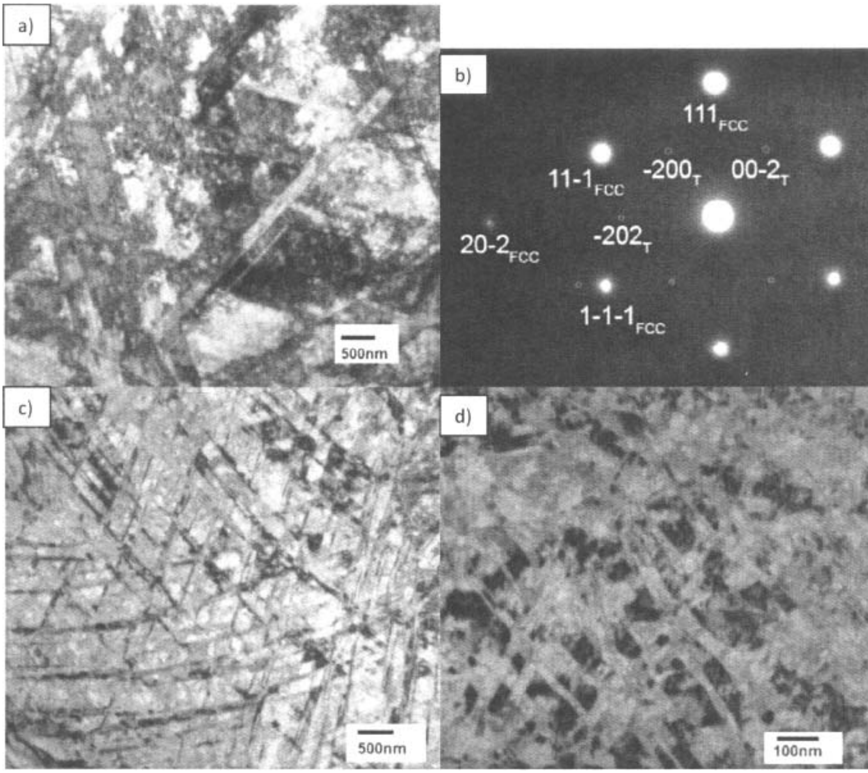

Figure 6 Bright field TEM images of samples after a) 30%CW, b) SAD diffraction pattern of a), c) 50%CW and d) 90%CW. Diffractions of twins are highlighted in b) for clear view.

were also seen in the heavily deformed samples, but not in large quantity. Further increase the cold work increased the number of deformation twins as shown in Fig.6d. Similar to [11], no *HCP* phase was identified in all cold worked samples. The aged samples have almost the same microstructures as the cold worked samples, but appears to have more micro-twins. Again, no *HCP* precipitates were found in all aged samples.

The 2D X-ray diffraction images of materials with different amount of cold work before and after aging are shown in Fig.7. Evidently, no significant difference can be seen among all samples; intensity pattern maintained the same, and no extra peaks showed up, confirming the TEM observations that no *HCP* precipitates were produced by heavy cold work or aging treatment. Fig.8 shows inverse pole figures of two heavily cold worked samples before and after aging. A strong <111> and a weak <100> texture was seen in the cold drawn condition, in agreement with that reported in [6]. Comparison between Fig.8a and 8c suggests that texture strength was increased by cold work. As both <111> and <100> orientations are unfavorable for dislocation slip [23], the strengthening of such texture distribution during cold drawn process also increased the mechanical strength. After aging, the <111> intensity in the 75%CW sample

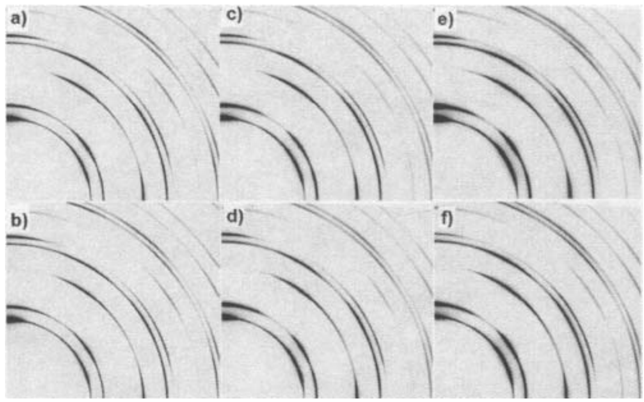

Figure 7 Synchrotron X-ray diffraction images of MP35N cold worked and aged samples: a) 30%CW, b) 30%CW, aged at 600°C/16hrs, c) 75%CW, d) 75%CW, aged at 500°C/16hrs, e) 90%CW and f) 90%CW, aged at 600°C/8hrs.

was increased, but it was slightly decreased in the 90%CW sample. While the <100> intensity spears to have an opposite trend.

From above, it is clear that MP35N deforms by the combination of dislocation slip and deformation twinning, and the stress induced *HCP* phase transformation plays no role during the room temperature deformation. The large work hardening of this material is related to the increased density of dislocations, intersection of planar deformation bands, the development of <111> and <100> texture, and the deformation twins, which decrease the grain size and also act as barriers to dislocation slip. This is consistent with other previous researches [11-13]. For the age hardening, since no HCP phase was identified in any of the aged sample by TEM or synchrotron X-ray diffraction, the mechanism proposed by S. Asgari et al. [8] doesn't apply to our case. Compare to those shown in [8], it is noted that the microstructure in this study shows mush less stacking faults at the similar cold work level (see Fig.6a), also the width of stacking fault was very thin. At higher cold work level (Fig.6d), no clear stacking faults were seen. This observation suggests that the material used in this study may have higher stacking fault energy, and thus different secondary strengthening mechanism compared to the material used in [8]. However, since the chemical composition was not listed in [8], no conclusion can be made at this moment. According to S. Asgari et al. [8], the dense and wide stack faults play a critical role in the formation of the HCP phase, lacking of heavily packed stacking fault in the cold worked condition could explain the absence of HCP phase after aging in this study. The large age hardening should have other causes. Although Fig.8 shows some differences in texture after aging, no clear pattern can be found at this moment as different trends were seen from samples with different amount of cold work. It is worth to note that Fig.8 shows the reconstructed textures based on the Rietveld refinement embedded in Maud software [21]. Although overall good fits were obtained, a 100% match the experimental results still remain challenging, especially for materials with sharp textures. A direct texture measurement by EBSD is recommended in that it may reveal some clues that weren't disclosed by Maud software.

As previously mentioned, although the microstructures in samples before and after aging are very similar, more micro-twins (with size in several nanometers) appeared to be formed during the aging process. The high stored energy caused by the homogeneous distribution of dislocations, stacking faults gives a high driving force for the formation of micro-twins. N. Jia, et al. [24] have studied the anomalous hardening behavior during annealing of a heavily deformed Cu and attributed it to the increased twinning boundaries and internal strains caused by the recovery of the deformation induced micro-twins. For FCC metals with high stacking fault energy like Ni, they gave the credit for the anomalous annealing hardening to the increased twin boundaries, which strength the material by decreasing the grain size and also acting as dislocation barriers [25]. To compare the internal strains between the cold worked and aged samples, X-ray diffraction spectra in the axial direction (±5 degrees) were interpreted by Williamson–Hall model assuming an isotropic strain distribution [26]. Some of the results are plotted in Fig.9. The internal strain is represented by the slope of the lines and y-intercept is related to the inverse of grain size. It is shown that the internal strain in the aged sample is lower than that in the cold worked sample probably due to the dislocation annihilation during aging heat treatment. However, the grain size appears to be decreased by aging, which is in agreement with the TEM observation. Therefore, the mechanism for the annealing hardening of Ni alloys [25] probably plays the same role in the heavily deformed MP35N alloy during aging. For the future study, a comprehensive and quantitative study the evolution of micro-twins using the high resolution TEM is recommended.

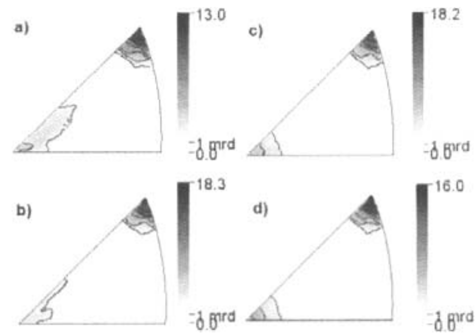

Figure 8 Inverse pole figures of samples with a)75%CW, b) 75%CW, 500°C/16hrs, c) 90%CW and d) 90%CW, 600°C/8hrs.

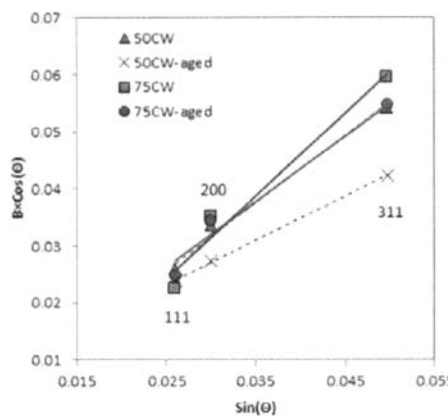

Figure 9 WH plot of the cold worked and aged samples.

CONCLUSIONS

The influence of cold work and aging treatment on the mechanical properties of MP35N was studied. It is found that this material work hardened rapidly with strength almost doubled after 30% cold work. Aging provides a secondary strengthening, which depends on the aging temperature and previous cold work level. An excellent combination of mechanical properties can be obtained from the material with 75%cw and aged at ~500°C for 2-4 hours, where the Y.S larger than 2000MPa, the UTS above 2200MPa and RA ~40% can be achieved. TEM observation and synchrotron X-ray diffraction suggest the work hardening is caused by the increased density of dislocations, the development of <111> and <100> texture, and deformation twins, while the secondary age hardening is associated with the increased number of micro-twins produced during the aging process.

ACKNOWLEDGEMENTS

The synchrotron X-ray diffraction was carried out ON beam line 11-ID-C at the Advanced Photon Source (APS) at Argonne National Laboratory. S. Cai would like to thank a Ph.D. student, S.J. Hao, for his assistant with the x-ray diffraction; and his colleagues S. Paul, K. Henry and T. Schumm for making samples. The support from Fort Wayne Metals management is greatly appreciated.

REFERENCES

1. G.D. Smith, US patent No 3,356,542, Dec. 1967
2. S. Asgari, Journal of Materials Processing Technology 155–156 (2004) 1905–1911
3. Carpenter datasheet, http://cartech.ides.com/datasheet.aspx?i=101&e=3&c=TechArt
4. Escalas F, Galante J, Rostoker W, Coogan PH. J Biomed Mater Res. 1975 May;9(3):303-13
5. D.M. Devine, M. Leitner, S.M. Perren, L.P. Boure and S.G. Pearce, European Cells and Materials, 18, 2009, pp.40-48
6. B.Q. Li and T.Steigauf, Proceeding of MPMD 2007, Palm Desert, California, USA, pp.120-123
7. E.M. Shaji, S.R. Kalidindi and R.D. Doherty, Mater. Sci. Eng., 272, 1999, 371-379
8. S. Asgari, E. El-Danaf, E. Shaji, S.R. Kalidindi and R.D. Doherty, Acta Mater., 46, 1998, pp.5795-5806
9. A.H. Graham and J.L. Youngblood, Metall. Trans., 1, 1970, 423-430
10. R. P. Singh and R.D. Doherty, Metall. Trans., 23, 1992, 307-319
11. S. Asgari, E. El-Danaf, S.R. Kalidindi and R.D. Doherty, Metall. Mater. Trans., 28, 1997, p.1781
12. M. Raghavan, B.J. Berkowitz and R.D. Kane, Metall. Trans., 11, 1980, 203-207
13. M. Raghavan and B.J. Berkowitz, Scrip. Metall., 14, 1980, 1009-1012
14. A.H. Graham, Trans ASM, 62, 1969, PP.930-935
15. A. Ishmaku and K. Han, J. Mater. Sci., 39, 2004, 5417-5420
16. B.Q. Li, T.Steigauf, P. McIntyre and P. Sorensen, Proceeding of MPMD 2009, Minneapolis, Minnesota, USA, pp.111-114
17. Per Enghag, *Steel Wire Technology, Applied Materials Technology, Stortorget, Sweden, Repro Örebro University, 2003*
18. A. Ishmaku and K. Han, Mater. Chara., 47, 2001,139-148
19. H.-R. Wenk and S. Grigull, J. Appl. Cryst. 36 (2003) 1040
20. A.P. Hammersley, FIT2D V9.129 reference manual V3.1, ESRF internal report, 1998
21. L. Lutterotti, S. Matthies, H.-R. Wenk, A.S. Schulz and J.W.Jr. Richardson, J. Appl. Phys. 81 (1997) 594
22. A.C. Larson, R.B. Von Dreele, Report No. LAUR 86-748, Los Alamos National Laboratory, 1994
23. D. Dye, H.J. Stone and R.C. Reed, Current Opinion in Solid State and Materials Science 5 (2001) 31–37

24. N. Jia, Y.D. Wang, S.D. Wu, W.Z. Han, Y.N. Wang, J.N. Deng and P.K. Liaw, Scripta Mate. 54 (2006) 1247–1252
25. N. Jia, X. Zhao, D. Song, M.H. Zhou and Y.D. Wang, Mater Sci Eng A 527 (2010) 1143–1150
26. G.K. Williamson and W.H. Hall, Acta Metal 1 (1953) 22.